Effects of Multiple Sintering Parameters on the Thermal Performance of Bi-porous Nickel Wicks in Loop Heat Pipes

Y. Qu [a], K. Zhou [a], K.F. Zhang [a], Y. Tian [b]

[a] School of Chemical Engineering, China University of Petroleum, Qingdao 266580, China

[b] School of Engineering and Technology, University of Hertfordshire, Hatfield, AL10 9AB, UK

Abstract: The thermal performances of a water-saturated bi-porous nickel wicks in Loop Heat Pipe (LHP) including porosity, permeability, capillary pumping head and effective thermal conductivity (ETC) have been examined theoretically and experimentally, based on five key sintering parameters including the content of pore forming agent, compacting pressure, sintering holding time, sintering temperature and the particle size of pore forming agent. A total number of 16 orthogonal tests are carried out with five key sintering factors and four levels of each factor. The optimal level of five sintering factors is obtained from the point of acquiring the most desirable overall performance of bi-porous nickel wicks, which can be as the reference sintering process for bi-porous nickel wicks. ETC is an important parameter of thermal performance, and its experimental values were compared with eleven theoretical models. The results showed that ETC was mostly affected by the content of pore former: 1.9 and 2.2 times respectively compared to the effect of compacting pressure and sintering holding time. The degree of effects from sintering temperature and pore-former particle size is similar and small. Alexander model and Maxwell model, the two most commonly used models for ETC estimate of LHP porous wicks, respectively overestimated and underestimated the experimental results of bi-porous nickel wicks. In the porosity range of 0.5-0.7, an average of the Chernysheva & Maydanik model and the Chaudhary & Bhandari model was found to be the best fit to the experimental data, providing an accurate method to predict ETC values of water-saturated bi-porous nickel wicks of LHP.

Keyword: loop heat pipe; bi-porous wick; effective thermal conductivity; sintering parameters; porosity; permeability.

Highlights:

- Porosity, permeability, capillary pumping head and ETC of water-saturated bi-porous nickel wicks are experimentally measured.
- The sensitivity analysis of five sintering parameters is conducted.
- The suitability evaluation of eleven existing ETC models is performed.
- The optimal sintering process has been suggested from sensitivity analysis.
- A feasible method to estimate ETC is suggested in the porosity range of 0.5-0.7.

Article History: Received 4 November 2015, Revised 31 March 2016, Accepted 1 April 2016, Available online 22 April 2016**.** Please cite as:

Y. Qu, K. Zhou, K.F. Zhang, **Y. Tian**, "Effects of Multiple Sintering Parameters on the Thermal Performance of Bi-porous Nickel Wicks in Loop Heat Pipes", *International Journal of Heat and Mass Transfer* **99**, 2016, pp. 638–646, doi:10.1016/j.ijheatmasstransfer.2016.04.005.

Nomenclature

A	sectional area (m^2)	R	sensitivity
CC	compensation chamber	t	Time (s)
D	cluster size (m)	T	Temperature ($°C$)
d	particle diameter (m)	Greek symbols	
E	compacting pressure	ε	porosity
F	pore former particle size	θ	contact angle (rad
G	sintering temperature	μ	dynamic viscosity ($kg/(m{\cdot}s)$)
h/H	capillary pumping head (m)	ρ	density (kg/m^3)
I	sintering holding time	σ	surface tension coefficient (kg/m^2)
J	content of pore forming agent	Subscripts and superscripts	
K	Permeability (m^2)	bi	bi-porous/bi-disperse
k_{eff}/ETC	effective thermal conductivity ($W/(m{\cdot}K)$)	eff	effective
k_f	fluid thermal conductivity ($W/(m{\cdot}K)$)	i	Level No.
k_s	solid thermal conductivity ($W/(m{\cdot}K)$)	j	Factor No.
m	mass (kg)	mono	mono-porous
R_{eff}	effective pore radius (μm)	w	wick

1. Introduction

Loop Heat Pipe (LHP) is a kind of high-efficient two-phase closed-cycle heat transfer system using capillary pumping principles. Porous wick is the key component in LHP evaporator by providing the driving force for circulation of the working fluid. With recent research and developments of compact LHP, new structures of porous wicks are increasingly being adopted to cope with highly intense heat flux used in high performance LHP. When heat flux is above 300 W/cm^2, conventional mono-porous wick cannot cope with the intense boiling and gas-liquid interactions and will cause system failure by having a dry-out wick. To solve the problem, bi-disperse/bi-porous wicks have been developed for LHP evaporators due to their superior performance: there are two size pore scales distribution with the large pores providing quicker escape path of vapor at high heating load, and with the small pores improving the capillary pumping to facilitate the working liquid to circulate to nucleation sites and increase the menisci area for evaporation.

Two commonly used dual-pore structures in LHP evaporator are the metal powder sintering type and the silicon lithography type. The former is usually used in cylinder evaporators while the latter is for plate type evaporators. Based on pore forming method, the metal powder sintering type can be subdivided into bi-porous structure and bi-dispersed structure. Bi-dispersed porous structure is composed of a macro-level cluster which is formed by agglomeration of micro-level particles, where the large pores are formed by heating the cluster binders to decomposition while the small pores are formed by sintering powder particles. Detailed information of the bi-dispersed structure manufacturing process was provided by Lin et al. [1]. Determination of key thermo-physical parameters of the bi-dispersed structure was

studied [2-4] and the evaporative/boiling heat transfer and two-phase flow characteristics were investigated [5-7]. Bi-porous wick is obtained by sintering the mixture of metal powder and water-soluble pore forming agent. Large pores are created by dissolving the pore forming agent in sintered wick while small pores are formed by sintering powder particle. Due to the higher porosity and easier control of the size of large pores than those passively formed large pores in the bi-dispersed wick, the bi-porous wick is widely used in LHP and will be thoroughly investigated in the current study.

There are four key performance parameters for the bi-porous wick in LHP: porosity, permeability, capillary pumping head and effective thermal conductivity (ETC, k_{eff}). These parameters are strongly dependent on the metal powder sintering, which is a complex process affected by multiple factors. Yeh et al.[8] described the manufacturing procedures of bi-porous wick and made statistical experimental analysis of three fabrication factors which affect the heat transfer capacity with two levels each factor, which are particle size and volume content of pore forming agent, and sintering temperature. They found better heat transfer performances in their test ranges with higher volume content and smaller particle size of pore forming agent and higher sintering temperature.

From the heat flow network of LHP evaporator, the heat applied to the evaporator wall mostly evaporates the liquid inside, but the rest inevitably heats the liquid in compensation chamber (CC) through the CC wall and porous wick skeleton by heat conduction, which is called heat leakage --a troublesome problem causing LHP operation instability: temperature fluctuation, temperature hysteresis and even the wick dry-out. Heat leakage, to a great extent, depends on the ETC values of the porous wick used. ETC also indicates the thermo-hydraulic performance of LHP evaporator and CC - key to the capillary wick structure optimization, and its value is strongly related to porosity and permeability. Computation the ETC of porous wicks therefore becomes of great importance to analyze the LHP heat transfer performance and design optimal wick structure. A wide range of thermal conduction models have been developed to predict the ETC of two phase system through solid (k_s) and fluid thermal conductivities (k_f) and porosity (ε). Tavman [9] reviewed a few heat conduction models of porous media. The well-known models are the weighted arithmetic mean (heat transfer in parallel) and weighted harmonic mean (heat transfer in series) of two phase thermal conductivities, which are normally used to determine the upper and lower bounds of porous medium ETC but can often be inaccurate. Other advanced ETC models such as Maxwell-Eucken model [10], Krupiczka model [11], Woodside and Messmer model [12], Assard model [13], Chaudhary & Bhandari model [14], Alexander model [15], EMT model [16], Dunn & Reay model [17], are often used to predict the ETC of mono-porous wicks. However, there exist very few previous studies on evaluating existing ETC models for bi-porous wick and examining their prediction errors. In addition, the ETC models for LHP bi-porous wicks are very few. Semenic et al. [18] provided the relationship between thermal conductivity of bi-dispersed sintered copper wick and the diameter ratio of particles to

clusters; however, their results strongly depended on the test samples. Chernysheva and Maydanik [19] reported a correlation but it was only aimed for bi-porous copper wick.

From the literature review, existing research on effects of sintering factors on bi-porous wick performance has only provided a qualitative analysis with a few factors and low levels for each factor. The majority of the current ETC models aims for the mono-porous wick. The two relations for bi-porous wick are based on the sintered copper powder without considering other materials. The current research aims to investigate the effect of multiple sintering parameters on bi-porous nickel wick performance including structure, fluid flow and heat transfer, to comprehensively analyze five sintering parameters (each with four levels), which are recognized as the main influence factors by existing researches, to study the influencing degree of each sintering parameter on porosity, permeability, capillary pumping head, effective thermal conductivity by an orthogonal experiment, and to find out the ideal sintering process of bi-porous nickel wick composing of optimal level of five sintering parameters. To examine the existing eleven ETC models for bi-porous nickel wick, comparison was made between the experimental and calculated values to provide a feasible and handy method for estimation of the effective thermal conductivity of water saturated bi-porous nickel wick.

2. Experiment

The bi-porous wick samples were fabricated by sintering the nickel powder INCO T255 with the filamentary microstructure, high porosity and low packing density. The fabrication process mainly consists of five steps: a) Screening. Pore forming agent (pure NaCl in analytical grade) was sieved into four size range (≤38μm, 38-75μm, 75-100μm, 100-125μm). b) Dry mixing. The above graded pore forming agent and nickel powders were alternatively sieved into crucible to ensure fully blended. The contents of pore forming agent were controlled respectively at 15%, 20%, 25% and 30%. c) Compacting. The powder mixture in the graphite die were pressed respectively at four pressure set points (5Mpa, 10Mpa, 15MPa, 20MPa) using a self-made pressure-controlled punching machine. A certain sintering holding time was necessary once reaching each set pressure value to ensure the even pressure and density distribution of green compact. d) Sintering. The smaller pores of bi-porous wick were formed by sintering. Sintering temperature, sintering holding time and heating rate are programmable controlled using GSL-1400X sintering furnace with argon as protection gas. e) Poaching and drying. The larger pores of bi-porous wick were formed by dissolving the pore forming agents. The sintered bi-porous wick samples were firstly poached in deionized water and then repeatedly rinsed in ultrasonic cleaner to ensure the absolute dissolution of pore forming agent. The dry wick samples were ready to test after drying in drying oven over 20 hours.

Table 1 Five sintering parameters with different levels

Level \ Factor	E(MPa)	F(μm)	G(℃)	I(min)	J(%)
Level 1	5	≤38	650	30	15
Level 2	10	38-75	700	40	20
Level 3	15	75-100	750	50	25
Level 4	20	100-125	800	60	30

To investigate effects of different sintering parameters on LHP bi-porous wick, the orthogonal experiment was designed with five factors, the compacting pressure (E), the particle size of pore forming agent (F), sintering temperature (G), sintering holding time (I), the content of pore forming agent (J), each run at four levels, represented by a_i, b_i, c_i, d_i, e_i, i = 1,2,3,4, as shown in Table 1. A total of sixteen orthogonal tests ($L_{16}(4^5)$) are formed as shown in Table 2. Experimental tests of porosity, permeability, capillary pumping head, ETC are carried out for these sixteen bi-porous nickel wick samples. Two samples are sintered in each orthogonal test and the parameter of each sample is measured five times. The parameter final value is the average of two samples.

Table 2 Orthogonal tests of 5 factors and 4 levels

Sample \ Level \ Factor	E (MPa)	F (μm)	G (℃)	I (min)	J (%)
1	5	≤38	650	30	15
2	5	38-75	700	40	20
3	5	75-100	750	50	25
4	5	100-125	800	60	30
5	10	≤38	700	50	30
6	10	38-75	650	60	25
7	10	75-100	800	30	20
8	10	100-125	750	40	15
9	15	≤38	750	60	20
10	15	38-75	800	50	15
11	15	75-100	650	40	30
12	15	100-125	700	30	25
13	20	≤38	800	40	25
14	20	38-75	750	30	30
15	20	75-100	700	60	15
16	20	100-125	650	50	20

2.1 Porosity

The methods for porosity (ε) measurement of porous media are mainly optical metallography and a point counting technique (Underwood [20]), the mercury intrusion porosimetry method and the Archimedes method (also called density method), among which the Archimedes method shown in Eq. (1) is easily manipulative and low-cost. Therefore it is used in the current work:

$$\varepsilon = \frac{(m_1 - m_3)/\rho}{(m_2 - m_3)/\rho} = \frac{m_1 - m_3}{m_2 - m_3} \tag{1}$$

where m_1 is the beaker mass with distilled water; m_2 is the total beaker mass when the wick sample is suspended in water and completely saturated; m_3 is the beaker mass when the saturated wick is removed from water and there is no water-drop dripping outside the beaker; ρ is the density of distilled water. All the above mass

quantities were measured within the accuracy of ± 0.1mg.

2.2 Permeability

Permeability indicates the fluid flow transport capacity through porous structure. For low velocity flow (<2.5cm/s) in saturated porous medium, permeability can be calculated by the Darcy's Law. However for the conditions such as high flow velocity, multiphase flow, heterogeneous fluid, compressible fluid, space-variation porosity etc., Darcy theory is not suitable and the Blake-Kozeny equation as Eq. (2), is widely used to calculate the permeability of saturated porous medium packed bed of spheres with diameter *d* and porosity ε.

$$K = \frac{d^2 \varepsilon^3}{150(1-\varepsilon)^2} \tag{2}$$

Carman-Kozeny equation has the similar form to Blake-Kozeny equation, except for the constant in denominator (180 instead of 150). In view of the complexity of porous structure, it is hard to evaluate the two equations above.

For bi-porous wick, permeability is difficult to measure due to the complex pore size distribution and uneven particle contacts and packing modes. Yu and Cheng [3] proposed a fractal permeability model for bi-dispersed porous media, which is limited because both the fractal dimensions of pore and the tortuosity are difficult to obtain accurately. Chen et al. [6] found that the permeability of sintered bi-dispersed porous medium can be estimated as the permeability of mono-dispersed porous medium having the same pore diameter as the macro-pore diameter of the bi-dispersed porous medium. Semenic et al. [18] measured the permeability of the sintered copper bi-porous slugs with silicone oils and yielded a linear regression formula for liquid and vapor permeability, which strongly depended on the test samples. Byon and Kim [21] pointed out three capillary flow regimes in bi-dispersed wick depending on the ratio between particle and cluster sizes (*d/D*) and developed different predicting correlations for the permeability of bi-dispersed wicks through finite element simulations.

When $0.125 < d/D < 0.7$ (Regime 1), the permeability of bi-dispersed wick is calculated by Eq. (3)

$$K_{bi} = \frac{\varepsilon^3 D^2}{150(1-\varepsilon)^2}\left[1 + 4.03\exp\left(3.29\frac{d}{D}\right)\left(\frac{d}{D}\right)^2\right] \tag{3}$$

When $d/D > 0.7$ (Regime 2), the permeability of bi-dispersed wick can be estimated like mono-dispersed porous medium: using Eq. (2), that is the first term on the right hand side of Eq. (3).

When $d/D < 0.125$ (Regime 3), the permeability of bi-dispersed wick is calculated by the second term on the right hand side of Eq. (3).

In our experiment, the T255 nickel powder particle size is about 4μm，the diameter ratio between nickel powder particle and pore forming agent particle is about 0.032 <

d/D < 0.1 when the particle size of pore forming agent is in the level 2-level 4 as shown in Table 1. When the particle size of pore forming agent is in the level 1, d/D > 0.125. Hence, Eq. (3) and the second term on the right hand side of Eq. (3) are used to calculate the permeability of each bi-porous wick sample in our study.

2.3 Capillary pumping head

Capillary performance of porous medium can be represented by the rising height of liquid interface in capillary tunnel. Within the same time scale, the higher the liquid interface is, the better the capillary performance is.

According to Washburn's equation [21] for capillary structures of effective pore diameters less than 300 μm where the inertia effect and gravity effect are negligible, the capillary pumping head can be calculated by Eq. (4)-(5).

$$h = \sqrt{\left(\frac{4\sigma}{\varepsilon\mu}\right)\left(\frac{K}{R_{eff}}\right)t} \tag{4}$$

$$R_{eff} = \frac{d}{2.094 + 2.824\cos\theta} \tag{5}$$

where σ is the surface tension coefficient; R_{eff} is the effective pore radius, which is equal to 0.205d when the contact angle θ is zero [22]. Substituting Eq. (3) and Eq. (5) into Eq. (4) leads to Eq. (6.1).

$$h = \frac{\varepsilon}{1\text{-}\varepsilon}\sqrt{\frac{19.672\sigma D}{150\mu}\left[1 + 4.03\exp\left(3.29\frac{d}{D}\right)\left(\frac{d}{D}\right)^2\right]t} \tag{6.1}$$

Substituting the second term on the right hand side of Eq. (3) and Eq. (5) into Eq. (4) leads to Eq. (6.2).

$$h = \frac{\varepsilon}{1-\varepsilon}\cdot\sqrt{\frac{D^2\cdot\left(2.094 + 2.824\cos\theta\right)}{150d}\cdot\frac{4\sigma}{\mu}\left[4.03\exp\left(3.29\frac{d}{D}\right)\left(\frac{d}{D}\right)^2\right]\cdot t} \tag{6.2}$$

The calculated values from Eq. (6.1) – (6.2) substituted into the experimental values of porosity ε are used for fitting our experimental values.

The schematic of capillary pumping performance test is shown in Fig.1. Each wick sample is fixed once the sample bottom perpendicularly touches the distilled water surface in the beaker. The beaker is placed on the analytical balance with accuracy of $\pm$ 0.1mg. As the capillary suctions, the liquid rises along the wick sample. The reading differences of balance before and after the wick sample bottom touching the liquid varied as a function of time, representing the capillary pumping mass rate. The correlation between the height of liquid interface and the capillary pumping mass is as follows:

$$h = \frac{m}{\rho\cdot A_w\cdot\varepsilon} \tag{7}$$

where m is the capillary pumping mass and A_w is the sectional area of the wick sample.

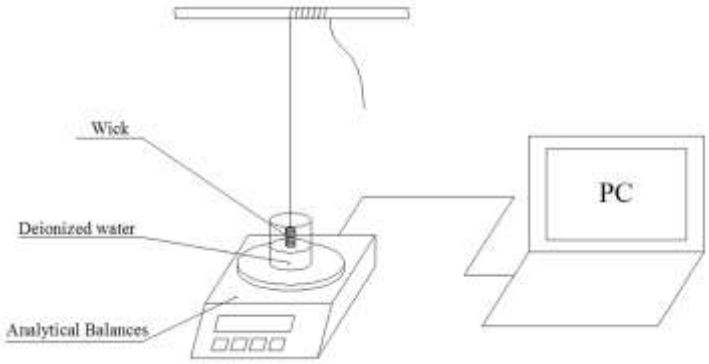

Fig. 1 Schematic of the capillary pumping test for bi-porous wicks

2.4 Effective thermal conductivity

A simple test rig was designed according to the Fourier's law of heat conduction to measure the ETC of 32 sintered nickel bi-porous samples in 16 orthogonal tests. As shown in Fig.2, the water saturated test sample vertically sandwiched between two copper blocks of the same cross section was fixed by clips and immersed in an ice-water mixture in the crucible container at the bottom end. The top end was attached to an electrical film heater. Silicone grease was applied at the contact surface to decrease the thermal resistance. The test system was wrapped by rock wool insulation material to prevent heat dissipation. The layout of eight copper constantan thermocouples was shown in Fig.2.

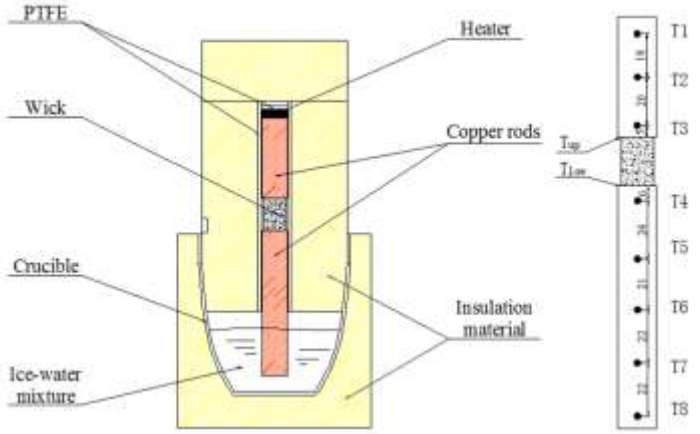

Fig. 2 Test schematic of effective thermal conductivity of bi-porous wick

The temperature of each measure point was recorded by the data acquisition system Agilent 34972A when heat transfer was steady. The steady heat transfer was defined as the temperature changes by less than 0.1 ℃ within 30 *s* and stayed steady for 10 *mins* at least. The effective thermal conductivity of water saturated bi-porous nickel sample can be obtained by Eq. (8) - (10).

$$k_w = \frac{k_{Cu} A_{Cu} h_w}{6A_w \cdot \left(T_{up} - T_{low}\right)} \cdot \sum_{i=1, i\neq 3}^{7} \frac{T_i - T_{i+1}}{\Delta x_{i-(i+1)}} \tag{8}$$

$$T_{up} = \frac{T_2 - T_3}{\Delta x_{2-3}} \cdot \Delta x_{3-up} + T_3 \tag{9}$$

$$T_{low} = \frac{T_4 - T_5}{\Delta x_{4-5}} \cdot \Delta x_{low-4} + T_4 \tag{10}$$

where T_{up} and T_{low} are the upper and lower end surface temperature ℃; h_w is the height of wick sample, m; k_{Cu} is the thermal conductivity coefficient of copper, $W/(m\cdot K)$; A_{Cu} and A_w are the cross section area of the copper and wick sample, m^2。 The uncertainty of temperature measurement is less than 5% with the uniform calibration using the standard mercurial thermometer.

3. Experimental Results and Discussion

3.1 Uncertainty analysis

For the directly measured quantity x_i, the uncertainty is calculated by the Bethel Eq. (11)-(12).

$$\hat{\sigma} = \sqrt{\frac{1}{n-1}\sum_{i=1}^{n}(x_i - \bar{x})^2} \tag{11}$$

$$\bar{x} = \frac{1}{n}\sum_{i=1}^{n} x_i \tag{12}$$

For the indirectly measured quantity Y_i, Eq. (13)-(15) is used.

$$\Delta Y = \frac{\partial F}{\partial x_1}\Delta x_1 + \frac{\partial F}{\partial x_2}\Delta x_2 + \ldots\ldots + \frac{\partial F}{\partial x_m}\Delta x_m \tag{13}$$

$$\begin{aligned}(\Delta Y)^2 = &(\frac{\partial F}{\partial x_1})^2(\Delta x_1)^2 + (\frac{\partial F}{\partial x_2})^2(\Delta x_2)^2 + \ldots\ldots + (\frac{\partial F}{\partial x_m})^2(\Delta x_m)^2 \\ &+2\frac{\partial F}{\partial x_1}\frac{\partial F}{\partial x_2}\Delta x_1\Delta x_2 + 2\frac{\partial F}{\partial x_1}\frac{\partial F}{\partial x_3}\Delta x_1\Delta x_3 + \ldots\ldots\end{aligned} \tag{14}$$

$$\sigma_y^2 = (\frac{\partial F}{\partial x_1})^2\sigma_1^2 + (\frac{\partial F}{\partial x_2})^2\sigma_2^2 + \ldots\ldots + (\frac{\partial F}{\partial x_m})^2\sigma_m^2 \tag{15}$$

$$\sigma_y = \sqrt{\alpha_1^{\,2}\sigma_1^{\,2} + \alpha_2^{\,2}\sigma_2^{\,2} + \ldots\ldots + \alpha_m^{\,2}\sigma_m^{\,2}} = \sqrt{\sum_{i=1}^{m}\alpha_i^{\,2}\sigma_i^{\,2}} \tag{16}$$

where $\alpha_i = \frac{\partial F}{\partial x_i}$ is the error transfer function. The uncertainties of porosity and

permeability were estimated to be $\pm 2\%$ and $\pm 3\%$, respectively .

3.1 Sensitivity and Optimal level analysis

The aim of sixteen orthogonal tests is to find the optimal level of each factor and the degree of sensitivity of five factors to four key parameters of sintered bi-porous nickel wick. y_{ji} is the average value of the four orthogonal test results with the i^{th} level of j^{th} factor. $y_{ji,k}$（k=1,2,3,4）represent the four test results of j^{th} factor at i^{th} level. Hence, the optimal level of the j^{th} factor is that corresponding to the maximum /minimum value of y_{ji}, i.e., the level of y_{ji} with the desirable value, which can be expressed in Eq. (17).

$$y_{ji}=\frac{1}{4}\sum_{k=1}^{4} y_{ji,k},\ i=1,2,3,4,\ j=a,b,c,d,e \tag{17}$$

The sensitivity of j^{th} factor impacted on the experimental results are represented as follows.

$$R_j = y_{j,max} - y_{j,min},\ j=a,b,c,d,e \tag{18}$$

Where R_j is the sample range of j^{th} factor. The higher value of R_j means the greater sensitivity.

Fig.3 shows the sensitivity analysis results of sintering parameters on four key parameters of bi-porous nickel wick. The sequences of impact degree of five sintering parameters are the same for porosity (ε), permeability (K) and capillary pumping head (H): the content of pore forming agent（J）>compacting pressure (E) > sintering temperature (G) >sintering holding time (I) > particle size of pore forming agent（F）. The largest effect factor is the content of pore forming agent (J). The reason is that the more content of pore forming agent, the larger amount of big pores created in bi-porous wicks, which facilitates vapor venting. For effective thermal conductivity, sensitivity analysis of existing eleven ETC models was carried out. The sensitivity of five sintering parameters (R value) are different, but the order of impact degree of five sintering parameters are the same: the content of pore forming agent (J) > compact pressure (E) > sintering holding time (I) >sintering temperature (G)> particle size of pore forming agent (F). The average impact degree of the largest effect factor, the content of pore forming agent, to compacting pressure (R_J/R_E) and to the sintering holding time (R_J/R_I) is 1.9 and 2.2 times, while the impact degrees of sintering temperature and the particle size of pore forming agent are comparable and relatively small. The value of R_J/R_E , R_J/R_I is the average computation valves of eleven models, where the subscript represents the impact factor.

Considering that sintered bi-porous nickel wicks should have the desirable comprehensive performance, the capillary pumping head (H), permeability (K), porosity (ε) should be selected as large as possible in the range of test values H = 3.3-5.8 mm in the 1*st* second of capillary suction, K = $(2.5\text{-}8.9)\times 10^{-14}$ (m^2), ε =0.5-0.7. The effective thermal conductivity to a great extend decides the heat leakage from LHP evaporator to compensation chamber and should be selected as small as possible due to nickel powder itself has higher thermal conductivity

compared with plastic material. Hence the optimal level of five sintering factors for sintered bi-porous nickel wick is that makes the capillary pumping head, the permeability and porosity maximum and makes the effective thermal conductivity minimum in the experimental ranges, that is, the compacting pressure E = 5*MPa*， the particle size of pore forming agent F ≤ 38*μm*， sintering temperature G = 650 ℃， sintering holding time I = 30*min*， the content of pore forming agent J = 30%, as shown in Table 3. The sintering process consisted of the optimal level of five sintering parameters can be as the reference for the manufacture of LHP bi-porous nickel wicks.

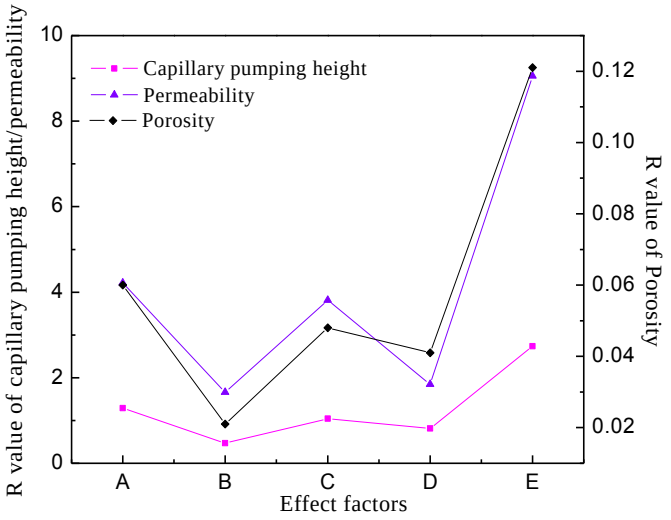

(a) Porosity/Permeability/Capillary pumping head

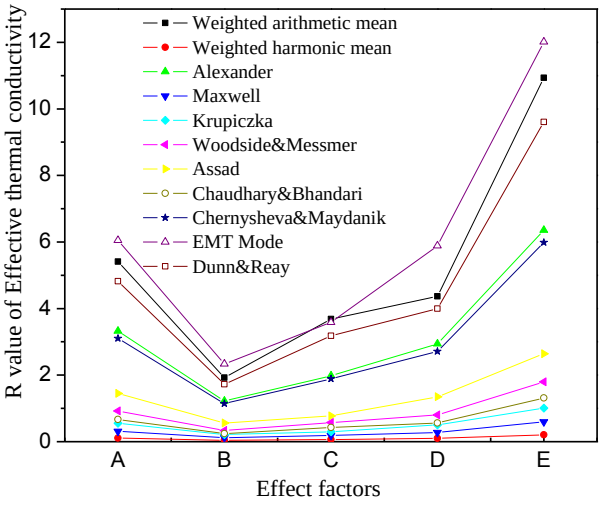

(b) Effective thermal conductivity

Fig. 3 Sensitivity analysis of sintering parameters on the key parameters of bi-porous wick

Table 3. Optimal level of five sintering parameters

	Compacting pressure (E)	Particle size of pore forming agent (F)	Sintering Temperature(G)	Holding time(I)	Content of pore forming agent(J)
Optimum level of y_j	5MPa	≤38μm	650℃	30min	30%

3.2 Effects of multi-sintering parameters on porosity and permeability

The changing curves of porosity and permeability of bi-porous nickel wick with four levels of five factors are shown in Fig.4. The average porosity of test samples are 55%-68%, which is a desirable range for LHP wicks. The content of pore forming agent, varying from 15% to 30% and making porosity increase by around 20% and permeability increase by around 2.5 times, becomes the largest effect factor to porosity and permeability of bi-porous nickel wicks among five sintering parameters. The particle size of pore forming agent and sintering holding time have relatively smaller effect on them. The variation trends of porosity and permeability of bi-porous nickel wicks with different levels of compacting pressure, sintering temperature, sintering holding time, the particle size of pore forming agent shown in Table 1, are the same, deceasing with the increase of above four sintering parameters, with the maximum reduction of 9.3% for porosity and 42.1% for permeability.

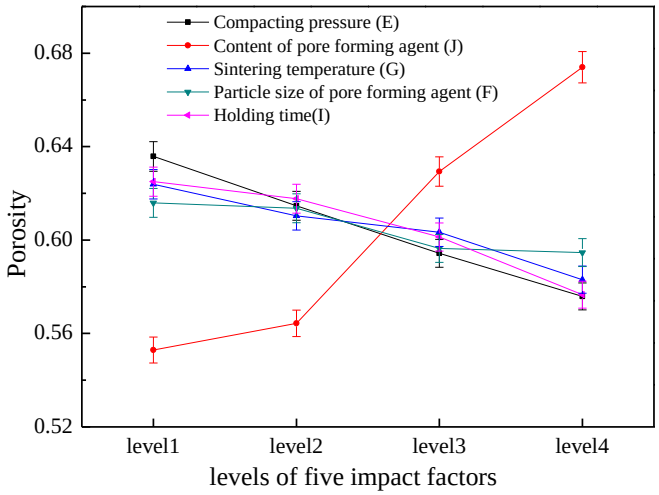

（a）Porosity

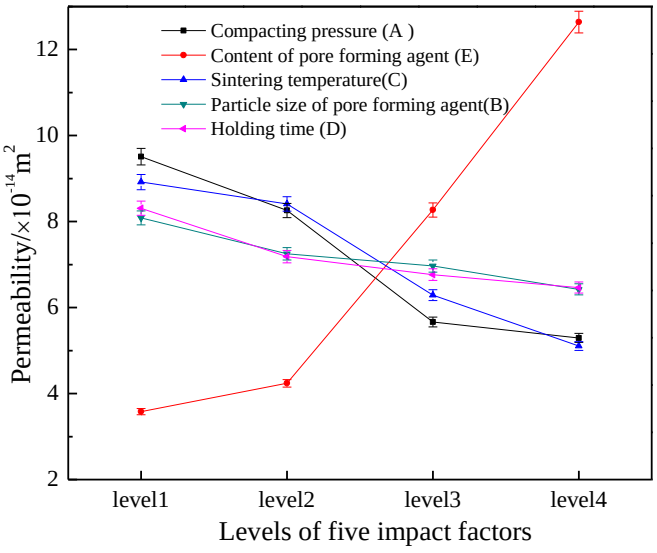

（b）Permeability

Fig. 4 Bi-porous wick (a) porosity and (b) permeability variation with sintering parameters

3.3 Effects of pore size on capillary pumping head

In salt-leaching pore forming method for fabrication bi-porous wicks, the macro-pore size mainly depends on the particle size of pore forming agent. Fig.4 indicates that the particle size of pore forming agent (F) has the smallest impact on the porosity of bi-porous wicks among five sintering parameters. The porosity is similar with different particle size of pore forming agent. Hence, for wick samples with same cross section, the higher of capillary pumping head at a certain time, the more mass intake and higher capillary suction rate. Fig.5 shows the pore size distribution of tested sintered bi-porous nickel wicks. The big pore is about 20μm.

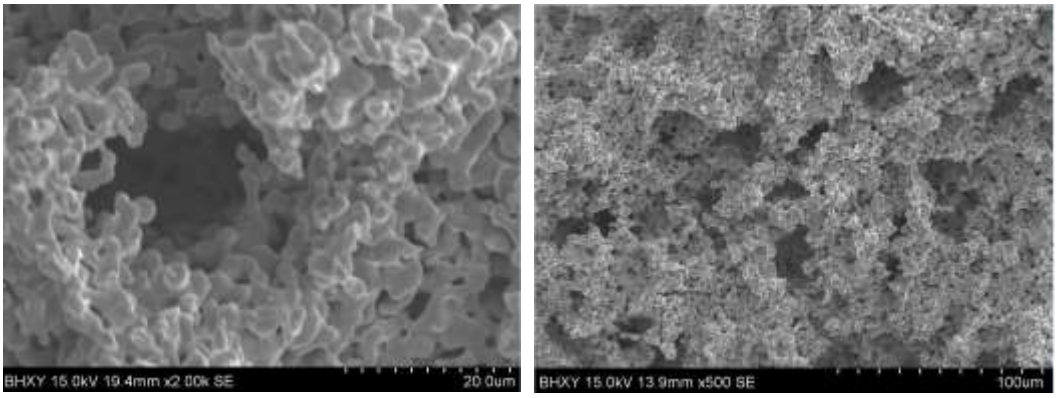

Fig. 5 SEM of bi-porous nickel wick with the particle size of pore forming agent of 19μm

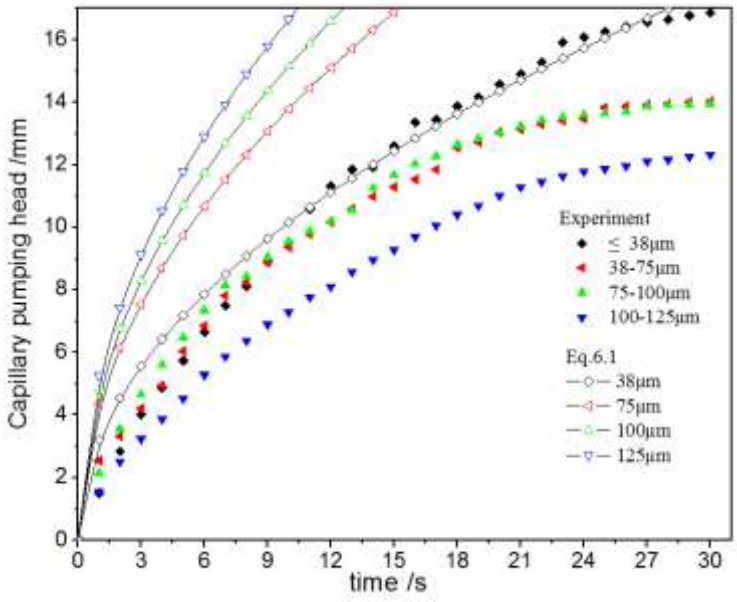

Fig. 6 Capillary pumping head comparison of experimental data with calculated data by Eq. (6.1)

In Fig.6, experimental data for capillary pumping head are compared with model for flow Regime 1 ($0.125 < d / D < 0.7$) represented by Eq. (6.1) within 30*s*, when nickel particle size is 4μm. With different particle size of pore forming agent, the computation curves by Eq. (6.1) display a large difference with the experimental value curves. When the particle size of pore forming agent is $D \leq 38$μm, the model by Eq. (6.1) predicts experimental results well within an error of 20%. As the particle size of pore forming agent increases, the deviation of the theoretical fitting from

experimental data enlarges. The reason is that, for $D \leq 38\text{um}$, the ratio between particle and cluster sizes is in the intermediate range ($0.125 < d / D < 0.7$), and flow is in Regime 1, in which large pores and small pores both contribute the capillary flow of bi-porous wicks. In the ranges of D=38~75μm,75~100μm, 100~125μm, d/D is small ($d / D < 0.125$), and flow is in Regime 3, the capillary flow proceeds mainly through small pores, whereas the large pores are not in favor of promoting fluid flow. Above results verified the optimum capillary performance regime suggested by Byon and Kim [21]. It also indicates that the pore forming agent particle size range should not be higher than 38μm in order to maximize the capillary performance, which is consistent with the optimized sintering process for bi-porous nickel wicks in Table 3.

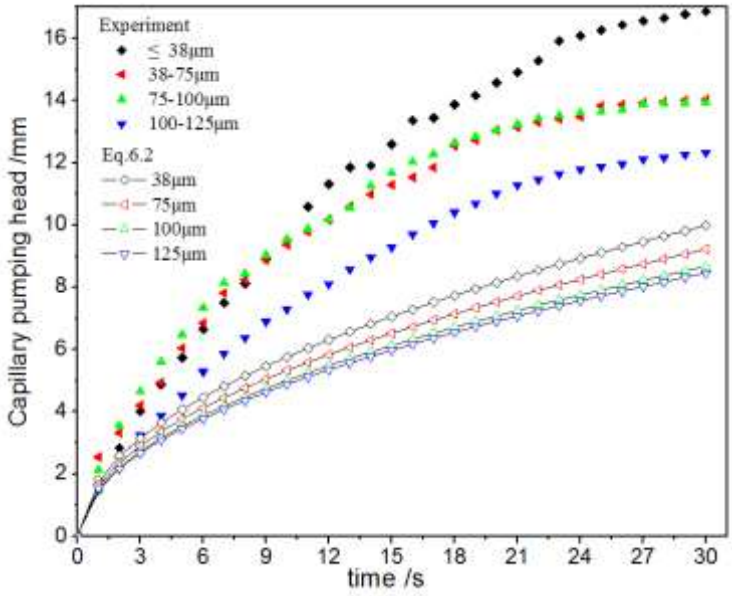

Fig. 7 Capillary pumping head comparison of experimental data with calculated data by Eq. (6.2)

Fig.7 gives the comparison results of experimental data with calculation values for flow Regime3 ($d / D < 0.125$) represented by Eq. (6.2). The results show that the model in Eq. (6.2) does not predict experimental results well. The underestimation is enlarged with the ratio between particle and cluster sizes decreases in the range of $d/D < 0.125$. The reasons are, firstly, Eq. (6.2) is based on the sintered glass particle wicks. In Regime 3, the capillary flow highly depends on the micro-pore surface effect. The surface effects of glass particles are obviously different with that of nickel particles. Secondly, the calculated values are based on the upper bounds of the particle size ranges of pore forming agent: $D = 38\text{~}75\mu\text{m}, 75\text{~}100\mu\text{m}, 100\text{~}125\mu\text{m}$. Meanwhile, the actual particle size of pore forming agent is smaller. Hence, the calculated value of d/D will be lower than the experiment values.

3.4 Effective thermal conductivity comparison analysis

Eleven ETC models are selected to make comparison analysis with the experimental values of sixteen group sintered bi-porous nickel wick samples. The calculation formulae of eleven ETC models are listed in Table 4. Fig. 8 shows the comparison results. In the porosity range of 0.5-0.7, five ETC models computation results are

closest approach to the experimental values, that is, Alexander model，Chernysheva & Maydanik model，EMT model，Assad model，Chaudhary & Bhandari model. Among them, Assad model and Chaudhary & Bhandari model underestimate the experimental values. Alexander model, as the most-used ETC model in LHP porous wicks, has the closest calculated curve with that of Chernysheva & Maydanik model, which is based on the LHP sintered bi-porous copper wicks. However, both models overestimate the experimental results.

Table 4. Effective thermal conductivity models for comparison

ETC Models	Expressions	ETC Models	Expressions
Parallel model (Max)	$k_{eff}=\varepsilon k_f+(1-\varepsilon)\ k_s$	Serial model (Min)	$\frac{1}{k_{eff}}=\frac{\varepsilon}{k_f}+\frac{(1-\varepsilon)}{k_s}$
Alexander Model	$k_{eff}=k_f\left(\frac{k_s}{k_f}\right)^{(1-\varepsilon)^{0.53}}$	Maxwell Model	$k_{eff}=k_f\cdot\frac{2\varepsilon k_f+(3-2\varepsilon)k_s}{(3-2\varepsilon)k_f+\varepsilon k_s}$
Krupiczka Model	$k_{eff}=k_f(k_s/k_f)^{\eta}$ $\eta=0.280-0.757\log\varepsilon-0.057\log(k_s/k_f)$	Assad Model	$k_{eff}=k_s\left(\frac{k_f}{k_s}\right)^{\varepsilon}$
Chernysheva& Maydanik Model	$k_{eff}=\frac{k_s(1-\varepsilon)}{(1+\varepsilon)^{2.1}}+\varepsilon\cdot k_f$	Dunn&Reay model	$k_{eff}=k_s\left[\frac{2+\kappa-2\varepsilon(1-\kappa)}{2+\kappa+\varepsilon(1-\kappa)}\right](\kappa=\frac{k_f}{k_s})$
Woodside&Messmer Model	$k_{eff}=\frac{(1.03-\varepsilon)k_s\cdot k_f}{k_s\left(1-\frac{1-\varepsilon}{1.03-\varepsilon}\right)+\frac{1-\varepsilon}{1.03-\varepsilon}\cdot k_f}+(\varepsilon-0.03)\cdot k_f$		
Chaudhary&Bhandari Model	$k_{eff}=\left(k_s(1-\varepsilon)+\varepsilon\cdot k_f\right)^n\left(\frac{k_fk_s}{k_f(1-\varepsilon)+\varepsilon\cdot k_s}\right)^{1-n}\ (0.42<n<0.51)$		
EMT Model	$k_{eff}=0.25\left\{(3\varepsilon\text{-}1)k_f+[3(1\text{-}\varepsilon)\text{-}1]k_s+\sqrt{[(3\varepsilon\text{-}1)k_f+[3(1\text{-}\varepsilon)\text{-}1]k_s]^2+8k_fk_s}\right\}$		

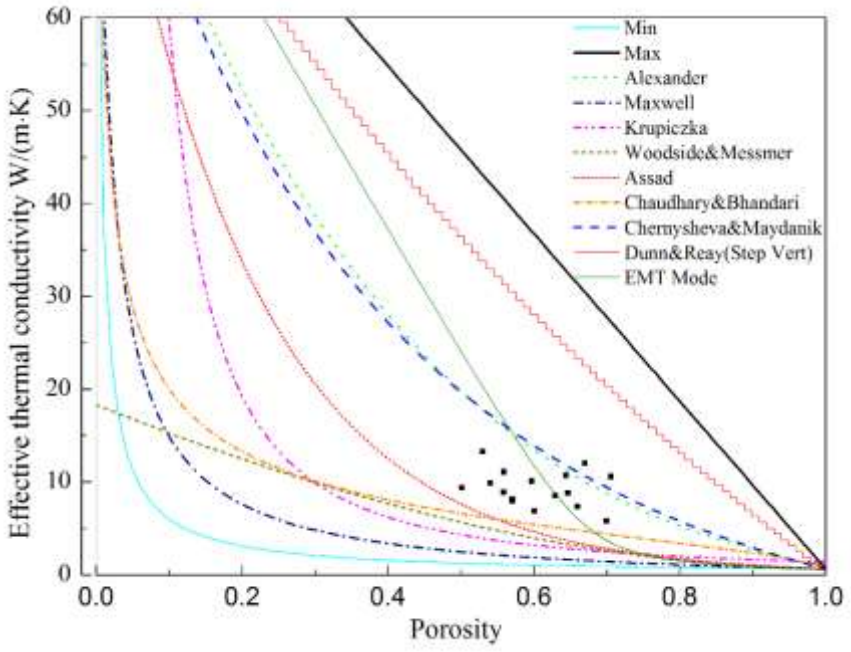

Fig. 8 Comparison of ETC experimental values and calculated values of bi-porous nickel wick

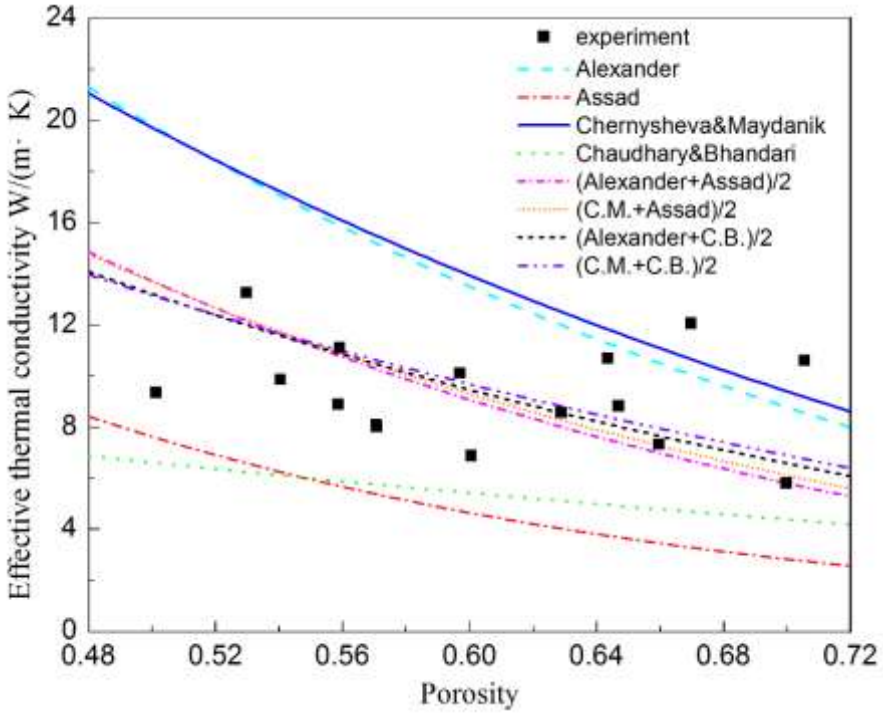

Fig. 9 Fitted curves of ETC bi-porous nickel wick

Carson et al. [16] pointed out that for porous medium composing of high thermal conductivity dispersed phase (such as air) and low thermal conductivity continuous phase (such as metal powders), the upper and lower bounds of effective thermal conductivity can be calculated using respectively EMT model and Maxwell-Eucken 2 model. Maxwell-Eucken 2 model is the Maxwell model that commonly used in LHP evaporator wicks. It is shown clearly in Fig.8 that Maxwell model, the lower bound suggested by Carson et.al., underestimates the effective thermal conductivity of sintered bi-porous nickel wicks, while EMT model, the upper bound suggested by Carson et.al., gives the better ETC estimation compared with Maxwell model although the degree of fitting of EMT model curve is not so desirable with the experimental points. This conclusion is also verified by the researches of Bodla et.al. [23] which indicate that EMT model is superior to Maxwell model for sintered powder porous medium due to the estimation error is only about 1/4 of the latter.

In order to seek an easy and feasible ETC prediction method that best fits the experimental values of bi-porous nickel wicks, the average curves of Assad-Alexander models, Chernysheva & Maydanick(C.M)-Assad models， Alexander-Chaudhary & Bhandari（C.B）models，and C.M-C.B models are made in Fig.9. The fitness of above four curves are respectively 0.925，0.930，0.939 and 0.941. It is clearly shown that the C.M-C.B models average curves best fits the experimental points. Hence, among the eleven ETC models, adopting the average of Chernysheva & Maydanick (C.M) and Chaudhary & Bhandari（C.B）models would be a simple but effective way to estimate the LHP water-saturated bi-porous nickel wicks.

4. Conclusion

1）For four key performance parameters of LHP bi-porous nickel wicks, which are porosity (ε), permeability (*K*), capillary pumping head (*H*) and effective thermal conductivity (ETC), the sensitivity analysis of five sintering parameters showed that the first two most influence factors for above four bi-porous wick properties, are the same, that is, the content of pore forming agent (J) and compacting pressure (E). For effective thermal conductivity, sensitivity analysis of existing eleven ETC models was carried out. The average impact index of the largest effect factor the content of pore forming agent to compacting pressure (R_J/R_E) is 1.9 times, while the impact degree of sintering temperature and pore former particle size are comparable and relatively small.

2）From the point of acquiring the most desirable overall performance of bi-porous nickel wick, the optimal levels of five sintering parameters are obtained, that is the compacting pressure E = 5 MPa，pore former particle size F ≤ 38μm，sintering temperature G = 650℃，sintering holding time I = 30min，the content of pore forming agent J = 30%, which can be the referenced sintering process of bi-porous nickel wicks.

3) The particle size of pore forming agent (F) has more influence on capillary pumping head than on porosity and permeability for bi-porous nickel wicks. The particle size range of pore forming agent should be D ≤ 38μm in order to maximize the capillary performance in the experimental ranges, in which the model shown in Eq. (6.1) predicts the experimental capillary pumping head results well within an error of 20%.

4）The suitability evaluation of existing eleven ETC models showed that the two most commonly used ETC models in LHP, the Alexander model and the Maxwell model, respectively overestimates and underestimates the experimental values of bi-porous nickel wicks. In the porosity range of 0.5-0.7, the average value of the Chaudhary & Bhandari model and the Chernysheva & Maydanik model best fits the ETC experimental values of water-saturated bi-porous nickel wicks, which would be a simple and feasible method to estimate the effective thermal conductivity of the LHP bi-porous nickel wicks.

Acknowledgments

This work is supported by the National Natural Science Foundation of China (NSFC Grant No.: 51206189) and the University of Hertfordshire (England, U.K.) through their Strategic Scientific Equipment Award (Grant No: 11.100824). The authors greatly appreciate their support.

References

[1] F.C. Lin, B.H. Liu, C.C. Juan, Y.M. Chen, Effect of pore size distribution in bidisperse wick on heat transfer in a loop heat pipe, Heat and Mass Transfer 47(2011) 933-940.

[2] Z.Q. Chen, P. Cheng, C.T. Hsu, A theoretical and experimental study on stagnant thermal conductivity of bi- dispersed porous media, International Communications in Heat and Mass Transfer 27(5) (2000) 601-610.

[3] B. Yu, P. Cheng, A fractal permeability model for bi-dispersed porous media, International Journal of Heat and Mass Transfer 45(2002) 2983-2993.

[4] B. Yu, P. Cheng, Fractal models for effective thermal conductivity of bidispersed porous media, Journal of Thermophysics and Heat Transfer 16(1) (2002) 22-29.

[5] F.C. Lin, B. H. Liu, C. T. Huang, Y.M.Chen, Evaporative heat transfer model of a loop heat pipe with bidisperse wick structure, International Journal of Heat and Mass Transfer 54(2011) 4621-4629.

[6] Z.Q. Chen, P. Cheng, T.S. Zhao, An experimental study of two phase flow and boiling heat transfer in bidispersed porous channels, International Communications in Heat and Mass Transfer 27(3) (2000) 293-302.

[7] X.L. Cao, P. Cheng, T.S. Zhao, Experimental study of evaporative heat transfer in sintered copper bidispersed wick structure, Journal of Thermophysics and Heat Transfer 16(4) (2002) 547-552.

[8] C.C. Yeh, B.H. Liu, Y.M. Chen, A study of loop heat pipe with biporous wicks, Heat and Mass Transfer 44(2008) 1537-1547.

[9] I.H. Tavman, Effective thermal conductivity of granular porous materials, International Communications in Heat and Mass Transfer 23(2) (1996) 169-176.

[10] J.C. Maxwell, A treatise on electricity and magnetism, 3rd ed., Clarendon Press, Oxford, England, 1904, Vol. 1, pp. 440.

[11] R. Krupiczka, Analysis of thermal conductivity in granular materials, International Journal of Chemical Engineering 7 (1967) 122-144

[12] W. Woodside, J.H. Messmer, Thermal conductivity of porous media – unconsolidated sands. Applied Physics 32(9) (1961) 1688-1699.

[13] A. Assad, A study of thermal conductivity of fluid bearing porous rocks. Berkeley, CA: University of California, 1955.

[14] D.R. Chaudhary, R.C. Bhandari. Thermal conductivity of two phase porous materials. British Journal of Applied Physics 2(1969) 609-610.

[15] G.P. Peterson, L.S. Fletcher. Effective thermal conductivity of sintered heat pipe wicks. Journal of Thermophysics and Heat Transfer 1(4) (1987) 343–347.

[16] J.K. Carson, S.J. Lovatt, D.J. Tanner, A.C. Cleland, Thermal conductivity bounds for isotropic, porous materials. International Journal of Heat and Mass Transfer 48(2005) 2150-2158.

[17] P.D. Dunn, D.A. Reay (Translated by H.Y. Zhou). Heat Pipes. Beijing: National Defence Industry Press, 1982.

[18] S. Tadej, L.Y. Yu, C. Ivan. Thermo- physical properties of biporous heat pipe evaporators. Journal of Heat Transfer-Transaction of the ASME 130 (2008) 1-10.

[19] M.A. Chernysheva, Y.F. Maydanik. Heat and mass transfer in evaporator of loop heat pipe. Journal of Thermophysics and Heat Transfer 23(4) (2009) 725–731.

[20] E. E. Underwood, Quantitative Stereology, Addison-Wesley, Reading, MA, 1970
[21] C. Byon, S.J. Kim, Capillary performance of bi-porous sintered metal wicks. International Journal of Heat and Mass Transfer 55(2012) 4096–4103.
[22] S.W. Chi, Heat pipe theory and practice. Hemisphere, Washington, 1976.
[23] K.K. Bodla, J.Y. Murthy, S.V. Garimella. Direct simulation of thermal transport through sintered wick microstructures. Journal of Heat Transfer-Transaction of the ASME 134(1) (2012) 012602.